# Relation Between Structure Functions and Cascade Rates in Anisotropic 2D Turbulence

Brodie C. Pearson,[a)] Jenna L. Pearson, and Baylor Fox-Kemper
*Department of Earth, Environmental and Planetary Sciences, Brown University, Providence, RI 02906, USA*

(Dated: 30 October 2019)

Relationships between second-order structure functions (blended from two different fields) and the cascade rates of enstrophy and kinetic energy are presented for the inertial forward enstrophy and inverse kinetic energy cascades of two-dimensional (2D) turbulence. These relationships are exact in homogeneous turbulence, and their evaluation does not require any assumption about the isotropy of turbulence. The second-order structure functions are not sign-definite, and their sign detects the direction (upscale or downscale) of the cascades. A corollary relation is derived for the enstrophy cascade, which relates the cascade rate to derivatives of another second-order structure function. Using a numerical simulation of 2D turbulence, the new structure functions are shown to be smoother than other commonly-used structure functions. The results are also discussed in the context of 2D flows with rotation, mean flow, forcing, and large-scale drag.

Keywords: Suggested keywords

One of the few exact laws of turbulence was derived for the inertial kinetic energy (KE) cascade of homogeneous, isotropic, incompressible three-dimensional (3D) turbulence[1]. This law is,

$$\overline{\delta u_L^3} = -\frac{4}{5}\epsilon_\nu r \tag{1}$$

where $\epsilon_\nu$ is the dissipation rate of kinetic energy by viscosity, $\delta\phi = [\phi(\mathbf{x}_0 + \mathbf{r}) - \phi(\mathbf{x}_0)]$ is the difference in a variable $\phi$ between two locations separated by the vector $\mathbf{r} = r\hat{\mathbf{r}}$, and $u_L = \mathbf{u}\cdot\hat{\mathbf{r}}$ is the longitudinal component of the velocity vector $\mathbf{u}$. The overline denotes an averaging operation, which could be over positions $\mathbf{x}_0$, angles, or time. The term on the left-hand side is the third-order longitudinal velocity structure function. Directly measuring $\epsilon_\nu$ (or equivalently the downscale cascade rate) is challenging because it requires measurements at viscous scales or regularly gridded data that can be spectrally transformed, but Eq. 1 provides a method to infer $\epsilon_\nu$ from the more easily observed structure function.

Equation 1 was proposed for isotropic turbulence[1], but a more general relation can be derived from the Karman-Howarth-Monin equations, governing the spatial autocorrelation of velocity components[2], which applies for anisotropic, but still homogeneous, turbulence,

$$\nabla_r \cdot \left[\overline{\delta\mathbf{u}(\delta\mathbf{u}\cdot\delta\mathbf{u})}\right] = -4\epsilon_\nu, \tag{2}$$

where $\nabla_r\cdot$ is the divergence in $\mathbf{r}$-space[3]. Equation 1 can be recovered by assuming isotropy, integrating Eq. 2 over a sphere of radius $r$, and using the divergence theorem. However, under anisotropic conditions Eq. 2 cannot be integrated without a detailed knowledge of the anisotropy, which is required to construct an appropriate volume of integration[4]. Several studies have integrated Eq. 2 in anisotropic, axisymmetric, 3D turbulence affected by rotation[5], stratification[6], and magnetism[4,7], but all these studies required assumptions be made about the volume of integration. Even if the appropriate volume is known, the resulting laws cannot be represented purely in terms of $u_L$[6], in contrast to Eq. 1.

A recent study[8] found that an alternative exact relationship exists for anisotropic, homogeneous 3D turbulence,

$$\overline{\delta\mathbf{u}\cdot\delta\left(\mathbf{u}\times\boldsymbol{\omega}\right)} = 2\epsilon_\nu, \tag{3}$$

where $\boldsymbol{\omega} = \nabla\times\mathbf{u}$ is the vorticity. Reassuringly, this same form holds in both non-rotating and constantly rotating coordinate frames, as $\overline{\delta\mathbf{u}\cdot\delta\left(\mathbf{u}\times\mathbf{f}\right)} = \overline{\delta\mathbf{u}\cdot\left(\delta\mathbf{u}\times\mathbf{f}\right)} = 0$, where $\mathbf{f}$ is the vorticity due to the rotating frame[8]. Eq. 3 provides a relationship between $\epsilon_\nu$ and a *second-order blended* structure function. That is, it is the product of two increments of differing fields. Equation 3 has two benefits over Eqs. 1-2. First, it applies under anisotropic conditions without requiring integration, and second, estimating second-order structure functions accurately typically requires less data than estimating third-order structure functions (see[9] and Section IV).

In contrast to 3D turbulence, two-dimensional (2D) turbulence can have two different inertial cascades; a downscale cascade of enstrophy $[\frac{1}{2}(\boldsymbol{\omega}\cdot\boldsymbol{\omega})]$ at rate $\epsilon_\omega$, and an upscale cascade of kinetic energy $[\frac{1}{2}(\mathbf{u}\cdot\mathbf{u})]$ at rate $\epsilon$. Note that $\epsilon$ is distinct from the viscous dissipation rate used in Eqs. 1-3, with $\epsilon_\nu$ being effectively zero in 2D turbulence for deep cascades[10] and having opposite sign to $\epsilon$ (as the KE fluxes in 3D and 2D turbulence are in opposing directions). In the upscale kinetic energy cascade of 2D turbulence Eq. 2 applies with $\epsilon$ replacing $\epsilon_\nu$. For *isotropic and homogeneous* 2D turbulence $\overline{\delta u_L^3}$ is proportional to $-\epsilon r$, as in Eq. 2 but with a different constant of proportionality[11,12] due to the 2D integration

surface being a disk rather than a sphere. In the enstrophy cascade of isotropic homogeneous 2D turbulence, the following laws apply[11,13],

$$\overline{\delta u_L^3} = \frac{1}{8}\epsilon_\omega r^3, \quad \text{and} \quad \overline{\delta u_L \delta\omega\delta\omega} = -2\epsilon_\omega r. \tag{4}$$

While the above equations don't apply in the enstrophy cascade of *anisotropic* 2D turbulence, a divergence law can still be formulated[13],

$$\nabla_r \cdot \left[\overline{\delta\mathbf{u}\delta\omega\delta\omega}\right] = -4\epsilon_\omega. \tag{5}$$

The evaluation of Eq. 5 in anisotropic flows is challenging for the same reasons as discussed for Eq. 2. These 2D relationships were originally developed to study large-scale geophysical systems[14–16], where often data is sparse and flows are anisotropic[17]. Therefore it would be useful to have an analogue of Eq. 3 for 2D turbulence, which depends on a second-order, rather than third-order, structure function and is insensitive to anisotropy.

The enstrophy cascade laws of Eqs. 4 and 5 are analogous to the energy cascade laws of Eqs. 1 and 2. However, there is currently no 2D turbulence version of Eq. 3 for either the enstrophy or inverse kinetic energy cascades. The aim of the present paper is to derive the former; a relationship between second-order structure functions and the enstrophy cascade rate, which applies under anisotropic conditions and does not require integration, thus bypassing the need for prior knowledge or assumptions about the anisotropy. In Section I we derive this relationship and its corollary, and we discuss the effects of mean flow and system rotation on the relation. The applicability of Eq. 3 to the inverse kinetic energy cascade of 2D turbulence is covered in Section II. In Section III the utility of the results are discussed, including their generalization to 2D systems with forcing or large-scale drag, their limitations and benefits versus existing relations for different data sets. In Section IV the new structure functions are diagnosed from a numerical simulation of 2D turbulence. The results are summarized in Section V.

## I. ENSTROPHY CASCADE OF 2D TURBULENCE

Two-dimensional, incompressible flows are governed by the vorticity equation,

$$\frac{\partial\boldsymbol{\omega}}{\partial t} + \mathbf{u}\cdot\nabla\boldsymbol{\omega} = \nu\nabla^2\boldsymbol{\omega}, \tag{6}$$

where $\boldsymbol{\omega}$ is vorticity, $\mathbf{u}$ is velocity, $\nu$ is viscosity, and $\nabla$ denotes derivatives with respect to position $\mathbf{x}$. For simplicity we shall initially consider a flow that consists only of turbulence, that is there is no mean flow ($\overline{\mathbf{u}} = 0$), however the results are unaffected by the presence of a constant mean flow ($\overline{\mathbf{u}} = \mathbf{U}_0$), as we shall discuss in Section I.A.

An equation for the spatial autocorrelation of vorticity $\overline{\boldsymbol{\omega}'\cdot\boldsymbol{\omega}}$, where $\boldsymbol{\omega} = \boldsymbol{\omega}(\mathbf{x})$ and $\boldsymbol{\omega}' = \boldsymbol{\omega}(\mathbf{x}+\mathbf{r}) = \boldsymbol{\omega}(\mathbf{x}')$ can be derived by multiplying Eq. 6 by $\boldsymbol{\omega}'$, and the analogous budget for $\boldsymbol{\omega}'$ by $\boldsymbol{\omega}$. Summing the resulting equations together and averaging gives,

$$\frac{\partial\overline{\boldsymbol{\omega}\cdot\boldsymbol{\omega}'}}{\partial t} + \overline{\boldsymbol{\omega}'\cdot(\mathbf{u}\cdot\nabla\boldsymbol{\omega})} + \overline{\boldsymbol{\omega}\cdot(\mathbf{u}'\cdot\nabla'\boldsymbol{\omega}')} = D_\omega(\mathbf{r}), \tag{7}$$

where

$$D_\omega(\mathbf{r}) = \overline{\boldsymbol{\omega}'\cdot(\nu\nabla^2\boldsymbol{\omega})} + \overline{\boldsymbol{\omega}\cdot(\nu\nabla'^2\boldsymbol{\omega}')} = 2\overline{\nu\nabla_r^2(\boldsymbol{\omega}\cdot\boldsymbol{\omega}')}, \tag{8}$$

$\nabla'$ denotes derivatives with respect to position $\mathbf{x}' = \mathbf{x}_0 + \mathbf{r}$, and we have used homogeneity and the fact that $\nabla \to \nabla_{x_0} - \nabla_r$ and $\nabla \to \nabla_r$ under the change of variables $\mathbf{x} = \mathbf{x}_0$ and $\mathbf{x}' = \mathbf{x}_0 + \mathbf{r}$[15,18] (see Appendix).

It is then convenient to define a variable which is equivalent in magnitude, but opposite in sign, to the advection of vorticity, $\boldsymbol{\mathcal{A}}_\omega = -\mathbf{u}\cdot\nabla\boldsymbol{\omega}$. In 2D dynamics, $\boldsymbol{\mathcal{A}}_\omega$ can also be written in several other forms. For example using vector identities it can be shown that,

$$\boldsymbol{\mathcal{A}}_\omega = \mathbf{u}\times(\nabla\times\boldsymbol{\omega}) = -\mathbf{u}\times\nabla^2\mathbf{u} = -\mathbf{u}\cdot\nabla\boldsymbol{\omega} = J(\omega,\psi), \tag{9}$$

where $J$ denotes the 2D Jacobian, and $\psi$ is the streamfunction of the flow. The utility of each of these formulations could vary for differing experimental setups, datasets, or numerical convenience, and the first formulation is similar to the Lamb vector ($\mathbf{u}\times\boldsymbol{\omega}$) in Eq. 3. With this variable, Eq. 7 and its single-point limit can respectively be written,

$$\frac{\partial\overline{\boldsymbol{\omega}\cdot\boldsymbol{\omega}'}}{\partial t} = \overline{\boldsymbol{\omega}'\cdot\boldsymbol{\mathcal{A}}_\omega} + \overline{\boldsymbol{\omega}\cdot\boldsymbol{\mathcal{A}}_\omega'} + D_\omega(\mathbf{r}), \quad \text{and} \tag{10}$$

$$\frac{\partial\overline{\boldsymbol{\omega}\cdot\boldsymbol{\omega}}}{\partial t} = \frac{\partial\overline{\boldsymbol{\omega}'\cdot\boldsymbol{\omega}'}}{\partial t} = 2\overline{\boldsymbol{\omega}\cdot\boldsymbol{\mathcal{A}}_\omega} - 2\epsilon_\omega, \tag{11}$$

where $\epsilon_\omega = \nu\overline{(\partial\omega_i/\partial x_j)(\partial\omega_i/\partial x_j)}$ is the enstrophy cascade rate (Einstein notation with repeated index summation implied) and we have used homogeneity ($\overline{\boldsymbol{\omega}\cdot\boldsymbol{\omega}} = \overline{\boldsymbol{\omega}'\cdot\boldsymbol{\omega}'}$ and $\overline{\boldsymbol{\omega}\cdot\boldsymbol{\mathcal{A}}_\omega} = \overline{\boldsymbol{\omega}'\cdot\boldsymbol{\mathcal{A}}_\omega'}$ ). Subtracting Eq. 10 from Eq. 11 and re-arranging we find,

$$\frac{\partial\overline{\delta\boldsymbol{\omega}\cdot\delta\boldsymbol{\omega}}}{\partial t} = 2\overline{\delta\boldsymbol{\omega}\cdot\delta\boldsymbol{\mathcal{A}}_\omega} - 4\epsilon_\omega - 2D_\omega(\mathbf{r}). \tag{12}$$

Assuming that there are a range of inertial cascade scales where turbulent statistics are stationary and $D_\omega(\mathbf{r}) \approx 0$,[13] we arrive at the following equation for the inertial enstrophy cascade of 2D turbulence,

$$\overline{\delta\boldsymbol{\omega}\cdot\delta\boldsymbol{\mathcal{A}}_\omega} = 2\epsilon_\omega. \tag{13}$$

This is the main result of this paper. This equation applies under anisotropic conditions, and does not require integration over a specific surface. It is analogous to Eq. 3 for 3D turbulence[8]. If the co-ordinate system is chosen such that vorticity is aligned with the vertical vector ($\hat{\mathbf{z}}$), then $\boldsymbol{\omega} = (0,0,\omega)$, $\mathbf{u} = (u,v,0)$, and the left-hand side of Eq. 13 can alternatively be written $-\overline{\delta\omega\delta(u\partial_x\omega + v\partial_y\omega)} = \overline{\delta\omega\delta\mathcal{A}_\omega}$. Note that the averaging, denoted by overlines, could be across multiple times, initial positions ($\mathbf{x}_0$), ensemble members, or directions (the latter could be affected by anisotropy).

Comparing Eqs. 13 and 5 it is apparent that the second- and third-order structure functions must be related by $\overline{\delta\omega\delta\mathcal{A}_\omega} = -(1/2)\nabla_r\cdot(\overline{\delta\mathbf{u}\delta\omega\delta\omega})$. This relationship can be validated by noting that,

$$\begin{aligned}\nabla_r\cdot(\overline{\delta\mathbf{u}\delta\omega\delta\omega}) &= \nabla_r\cdot(\overline{\mathbf{u}'\omega'\omega'}-2\overline{\mathbf{u}'\omega\omega'}-\overline{\mathbf{u}\omega'\omega'}+\overline{\mathbf{u}'\omega\omega}+2\overline{\mathbf{u}\omega'\omega}-\overline{\mathbf{u}\omega\omega})\\ &= -2\nabla'\cdot(\overline{\mathbf{u}'\omega\omega'})+\nabla\cdot(\overline{\mathbf{u}\omega'\omega'})+\nabla'\cdot(\overline{\mathbf{u}'\omega\omega})-2\nabla\cdot(\overline{\mathbf{u}\omega'\omega})\\ &= -2\overline{\omega\mathbf{u}'\cdot\nabla'(\omega')}-2\overline{\omega'\mathbf{u}\cdot\nabla(\omega)}=2\overline{\delta\omega\delta(u\partial_x\omega+v\partial_y\omega)}=-2\overline{\delta\omega\delta\mathcal{A}_\omega},\end{aligned} \tag{14}$$

where we have used co-ordinate transforms (Appendix A), incompressibility and homogeneity (i.e., $2\nabla\cdot(\overline{\mathbf{u}\omega\omega})=\overline{\omega\mathbf{u}\cdot\nabla\omega}=\overline{\omega'\mathbf{u}'\cdot\nabla'\omega'}=0$), but isotropy is not assumed or required.

### I.A. Effects of Rotation and Mean Flow

If a 2D turbulent system is rotating at a constant rate $\mathbf{\Omega}$, the fluid parcels are affected by a Coriolis acceleration. As a result, in a rotating system the vorticity budget (Eq. 6) becomes a budget for the absolute vorticity oriented out of the plane of motion ($\zeta=\omega+2\mathbf{\Omega}\cdot\hat{\boldsymbol{z}}$) which includes a Coriolis term $\nabla\times[\mathbf{u}\times 2\mathbf{\Omega}]$. However, noting that such systems obey governing equations identical to (6) except with $\omega\to\zeta$, the immediate equivalent to (13) is

$$\overline{\delta\boldsymbol{\zeta}\cdot\delta\boldsymbol{\mathcal{A}}_\zeta}=2\epsilon_\zeta,\qquad \boldsymbol{\mathcal{A}}_\zeta=-\mathbf{u}\cdot\nabla\zeta=\mathbf{u}\times(\nabla\times\boldsymbol{\zeta}). \tag{15}$$

The effects of system rotation on this relation can then be diagnosed; for example, for constant frame rotation ($f$-plane, $\boldsymbol{\zeta}=(\omega+f_0)\hat{\boldsymbol{z}}$) or tangent plane [$\beta$-plane, $\boldsymbol{\zeta}=(\omega+f_0+\beta y)\hat{\mathbf{z}}$] systems. For 2D motions on the surface of a rotating sphere [$\boldsymbol{\zeta}=(\omega+2\Omega\sin\theta)\hat{\mathbf{z}}$, $\theta$ is latitude] the scales of interest would need to be small enough that $\delta\boldsymbol{\zeta}$ and $\delta\mathcal{A}_\zeta$ are dominated by turbulent fluctuations rather than spatial variation of the local vertical direction ($\hat{\mathbf{z}}$).

It was stated at the start of the above derivation that Eq. 13 is valid in turbulent flows with a constant background velocity. The presence of a constant background mean flow $\mathbf{U}_0$, where $\mathbf{u}=\mathbf{u}_t+\mathbf{U}_0$ and $\overline{\mathbf{u}_t}=0$ is the turbulent velocity field, would lead to a term, $\mathbf{U}_0\cdot\nabla\boldsymbol{\omega}$, on the left-hand side of Eq. 6 (note that $\overline{\boldsymbol{\omega}}$ is still zero). As a result, Eq. 13 would have an additional term that, for a constant background flow, is zero;

$$\begin{aligned}\overline{\delta\boldsymbol{\omega}\cdot\delta\left(\mathbf{U}_0\cdot\nabla\boldsymbol{\omega}\right)} &= \mathbf{U}_0\cdot\nabla\left(\frac{1}{2}\overline{\boldsymbol{\omega}\cdot\boldsymbol{\omega}}-\overline{\boldsymbol{\omega}'\cdot\boldsymbol{\omega}}\right)+\mathbf{U}_0\cdot\nabla'\left(\frac{1}{2}\overline{\boldsymbol{\omega}'\cdot\boldsymbol{\omega}'}-\overline{\boldsymbol{\omega}'\cdot\boldsymbol{\omega}}\right)=-\mathbf{U}_0\cdot\nabla\left(\overline{\boldsymbol{\omega}'\cdot\boldsymbol{\omega}}\right)-\mathbf{U}_0\cdot\nabla'\left(\overline{\boldsymbol{\omega}'\cdot\boldsymbol{\omega}}\right),\\ &= \mathbf{U}_0\cdot\nabla_r\left(\overline{\boldsymbol{\omega}'\cdot\boldsymbol{\omega}}\right)-\mathbf{U}_0\cdot\nabla_{x_0}\left(\overline{\boldsymbol{\omega}'\cdot\boldsymbol{\omega}}\right)-\mathbf{U}_0\cdot\nabla_r\left(\overline{\boldsymbol{\omega}'\cdot\boldsymbol{\omega}}\right),=-\mathbf{U}_0\cdot\nabla_{x_0}\left(\overline{\boldsymbol{\omega}'\cdot\boldsymbol{\omega}}\right)=0,\end{aligned}$$

where we have used homogeneity and a coordinate transformation. Equation 13 is therefore not affected by a constant background flow. Equivalently it is Galilean invariant - unaffected by the relative velocities of the fluid and observational platforms. This is an important property for the interpretation of remotely-sensed data (e.g., satellite observations of the Earth).

### I.B. A corollary in the enstrophy cascade

In isotropic, homogeneous 2D turbulence, there are two relationships for the third-order structure functions in the enstrophy cascade (Eq. 4). In analogy to this, another second-order structure function relationship can be derived in addition to Eq. 13. The second-order vorticity structure function budget (Eq. 12) in homogeneous 2D turbulence can be written in several different forms, and comparing these different forms it is seen that $\overline{\delta\boldsymbol{\omega}\cdot\delta\boldsymbol{\mathcal{A}}_\omega}=-(1/2)\nabla_r\cdot\left[\overline{\delta\mathbf{u}(\delta\boldsymbol{\omega}\cdot\delta\boldsymbol{\omega})}\right]$ (Eq. 14), and $\overline{\delta\boldsymbol{\omega}\cdot\delta\boldsymbol{\mathcal{A}}_\omega}=(1/2)\nabla_r^2\left[\nabla_r\cdot\left(\overline{\delta\mathbf{u}\left(\delta\mathbf{u}\cdot\delta\mathbf{u}\right)}\right)\right]$[11] (their Eq. 12). For homogeneous (3D or 2D) turbulence it has also been demonstrated that $2\delta\mathbf{u}\cdot\delta\left(\mathbf{u}\times\boldsymbol{\omega}\right)=-\nabla_r\cdot\left(\overline{\delta\mathbf{u}\left(\delta\mathbf{u}\cdot\delta\mathbf{u}\right)}\right)$[8]. Equation 13 can then be written in an alternative form,

$$\nabla_r^2\left[\overline{\delta\mathbf{u}\cdot\delta\left(\mathbf{u}\times\boldsymbol{\omega}\right)}\right]=-2\epsilon_\omega. \tag{16}$$

Together, Eq. 13 and Eq. 16 provide relationships between second-order structure functions and the enstrophy cascade rate in the enstrophy cascade of 2D turbulence. These equations apply under anisotropic conditions, with the important benefit that Eq. 13 does not require integration, unlike existing relations (Eq. 5). While Eq. 16 does require integration, in the limit of isotropic turbulence it can be integrated over a disc to find,

$$\overline{\delta\mathbf{u}\cdot\delta\left(\mathbf{u}\times\boldsymbol{\omega}\right)}=-\frac{1}{2}\epsilon_\omega r^2. \tag{17}$$

The left hand-side of Eq. 17 can alternatively be written as $\overline{\delta\boldsymbol{u}\cdot\delta\boldsymbol{\mathcal{A}}_{\boldsymbol{u}}}$. Equations 16 and 17 can also be modified to account for the effects of a rotating system by changing $\boldsymbol{\omega}\to(\boldsymbol{\omega}+2\mathbf{\Omega})$. As in Eq. 13, this rotation effect is identically zero under solid body rotation.

## II. INVERSE KINETIC ENERGY CASCADE

In addition to an enstrophy cascade, 2D turbulence can also produce an inverse cascade of kinetic energy, where

'inverse' refers to the fact that kinetic energy moves from small scales to large scales. Except for the constraint that 2D flow only has two velocity components, the 2D and 3D Navier-Stokes equations are identical,

$$\frac{\partial \mathbf{u}}{\partial t} = -\mathbf{u}\cdot\nabla\mathbf{u} + \nu\nabla^2\mathbf{u} - \nabla\left(\frac{p}{\rho}\right) + \mathbf{f}_u$$
$$= \mathbf{u}\times\boldsymbol{\omega} + \nu\nabla^2\mathbf{u} - \nabla\left(\frac{p}{\rho} + \frac{\mathbf{u}\cdot\mathbf{u}}{2}\right) + \mathbf{f}_u, \quad (18)$$

where $p$ is pressure and $\rho$ is (constant) density.

The derivation of Eq. 3 for the forward kinetic energy cascade of 3D turbulence by[8] was derived from Eq. 18 by assuming statistical homogeneity and incompressibility, and *without* assuming isotropy. As a result, their derivation can be applied to 2D dynamics, that is,

$$\overline{\delta\mathbf{u}\cdot\delta\left(\mathbf{u}\times\boldsymbol{\omega}\right)} = 2\epsilon = -2P, \quad (19)$$

is also a constraint in homogeneous 2D turbulence, where $P = -\varepsilon$ is the upscale cascade rate of KE. Care should be taken to note that in the kinetic energy cascade of 2D turbulence, kinetic energy is transferred to large scales which means that $\epsilon$ and, as a result, $\overline{\delta\mathbf{u}\cdot\delta\left(\mathbf{u}\times\boldsymbol{\omega}\right)}$ are both negative[11]. This is in contrast to the kinetic energy cascade of 3D turbulence where both are positive[8] and kinetic energy is transferred to small scales where it is dissipated by viscosity. As recently discussed[8], in a rotating system $\boldsymbol{\omega}\rightarrow\boldsymbol{\omega}+\boldsymbol{\Omega}$ in Eq. 19, which has no effect under solid body rotation. They also found that if there is a mean velocity ($\mathbf{U}_0$) then there is an additional term on the left of Eq. 3 which takes the form $\overline{\delta\mathbf{u}\cdot\delta\left(\mathbf{U}_0\times\boldsymbol{\omega}\right)}$. In 2D turbulence this term must be zero as the velocity and vorticity vectors are perpendicular. Therefore Eq. 19 (and similarly Eq. 16) is applicable even if there is a constant mean velocity.

## III. UTILITY OF NEW RELATIONS

The above results were derived from the unforced vorticity budget (Eq. 6) with viscous damping. It is common for 2D turbulent systems to also be forced, often at a particular scale, or damped at large scales. Forcing can supply energy (enstrophy) for the inverse energy (direct enstrophy) cascade. Previous studies have found that the presence of external forcing at a specific scale does not affect the third-order structure function laws in the forward enstrophy and inverse kinetic energy inertial cascades of 2D turbulence[11,19], or the forward energy inertial cascade of 3D turbulence[8]. Following the above discussion of the links between third- and second-order structure functions (Sec. I.B) it follows that the presence of external forcing at a given scale should not affect the second-order structure function laws presented in this paper, providing the scales ($\mathbf{r}$) are within an inertial cascade. Similarly, large-scale drag should not affect the equations for the enstrophy cascade presented here, although it will reduce the down-scale enstrophy cascade rate $\epsilon_\omega$ as some enstrophy will be removed by drag at large-scales[19]. In contrast, these laws would need modification in systems with overlapping energy and enstrophy inertial cascades, which can arise from simultaneous small-scale kinetic energy forcing and large-scale enstrophy forcing[11] or from forced 2D turbulence with large-scale or scale-independent drag where enstrophy transfer to large-scales overlaps with the inverse kinetic energy cascade[19,20]. Third-order structure function laws have also been proposed for regions outside the inertial cascades in isotropic 2D turbulence[21]. The relationship shown in Eq. 14 means that any extant laws containing $\nabla_r\cdot(\overline{\delta\mathbf{u}\delta\omega\delta\omega})$ can be converted into laws in terms of $\overline{\delta\omega\delta\mathcal{A}_\omega}$, and similarly the relation[8] $\overline{\delta\mathbf{u}\cdot\delta\left(\mathbf{u}\times\boldsymbol{\omega}\right)} = -(1/2)\nabla_r\cdot(\overline{\delta\mathbf{u}[\delta\mathbf{u}\cdot\delta\mathbf{u}]})$ allows the conversion of extant laws with third-order velocity structure functions into laws with second-order structure functions. Together these relations can be used to convert the above-referenced results into second-order structure function laws.

The relationships derived above depend on second-order structure functions (where order is defined by the number of $\delta$ terms), and may therefore be expected to converge faster than their third-order counterparts[8]. However, this intuition follows from the fact that $\overline{\delta\phi\delta\phi}$ and $\overline{\delta\phi\delta\phi\delta\phi}$ are averages of positive-definite and dual-signed quantities respectively. The latter is therefore a residual and requires more data to converge than the former, particularly for variables that are almost symmetrically distributed such as turbulent velocity[9]. The second-order structure functions presented here are not positive-definite because they are blended structure functions of two different fields, for example $\delta\boldsymbol{\omega}$ and $\delta\boldsymbol{\mathcal{A}}_\omega$, which are not necessarily aligned, and the implications of this for convergence are not trivial. However, a numerical simulation of 2D turbulence, which will be discussed in the next section, suggests that the new structure functions do converge faster than other structure functions used to diagnose cascade rates. Differences in convergence could result from the differing mixtures of intervals ($\delta\phi$) and derivatives with respect to the relative ($\nabla_r$) or the absolute (i.e. $\omega$, $\nabla$) co-ordinates. Eq. 4 involves 2 $\omega$'s and three intervals; Eq. 5 involves a relative derivative, 2 $\omega$'s and three intervals; and Eq. 13 involves two $\omega$'s, an absolute derivative, and two intervals. A recent study[22] notes that in many cases an interval is just a definite integral of a derivative.

### III.A. Considerations for diagnosing the new relations

Third-order structure functions have previously been used to study the dynamics of the atmosphere and ocean[14,16,23,24]. However, making appropriate measurements of flow properties can be challenging due to the nature of both in situ and remote data collection away from the land surface[25–27]. Although second-order structure functions may require less data to converge with their mean value than third-order structure functions, the results presented here require products of flow properties and their derivatives (e.g. vorticity). For some

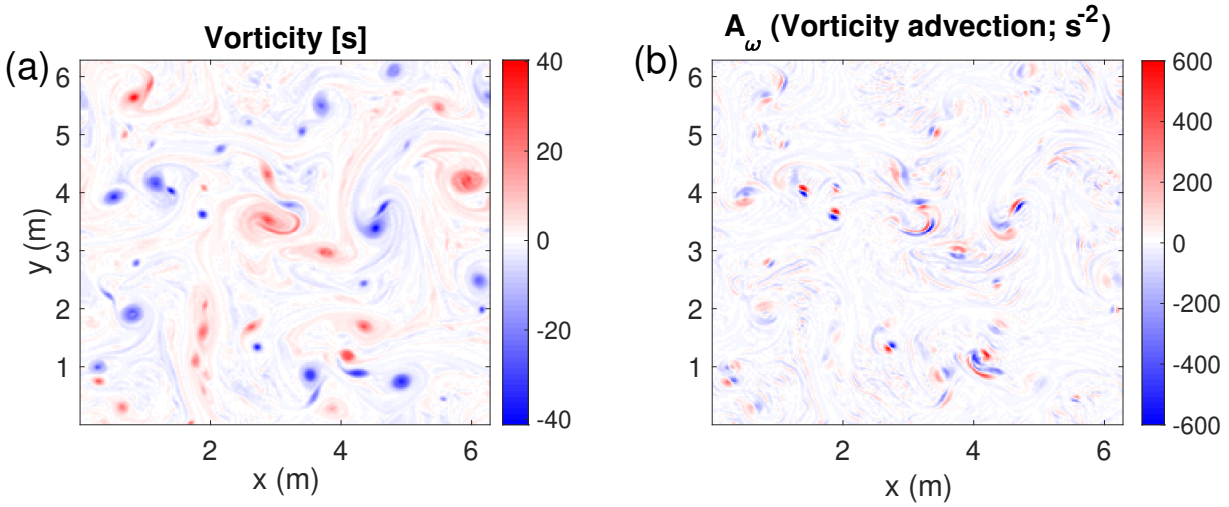


FIG. 1 Snapshots of (a) vorticity $\omega$ and (b) the vorticity advection term $\mathcal{A}_\omega$ for freely decaying 2D turbulence.

geophysical measurement techniques, such as aircraft-track data[11,16], this information is not available and the new structure functions may not be diagnosable. However, there are many current and future data sets where sufficient information is available to diagnose the new structure functions. For example in the ocean, platforms that can diagnose vorticity and gradients include surface drifter deployments[28], radar observations[29], and gridded satellite observations[30], and there is also significant potential for upcoming satellite campaigns[31]. Numerical simulations also provide the necessary variables to diagnose the new structure functions. Global-scale numerical simulations can presently resolve large-scale turbulence in both the atmosphere and ocean[32], and analyses of cascade rate statistics in these simulations, which could be inferred from structure functions, can improve our physical understanding of these systems[33].

## IV. COMPARISON OF NEW AND EXISTING RELATIONS USING A NUMERICAL MODEL

One way to test the utility of the new structure functions is by diagnosing them in a 2D turbulent flow, and comparing them to more commonly-used structure functions. To achieve this we carried out a numerical simulation of freely-decaying isotropic turbulent 2D dynamics using an open-source Python package, *pyqg*[34]. In 'barotropic' mode, this simulation solves the vorticity equation (Eq. 6) in a doubly-periodic square domain of width $2\pi$, with 256 grid points in each direction. This simulation follows a standard decaying turbulence setup[35], turbulence develops from the initial condition of the streamfunction $\psi$; a random field with a prescribed wavenumber spectrum of $|\hat{\psi}|^2 = A|k|\left[1+(|k|/6)^4\right]^{-1}$ where $A$ is chosen such that the initial non-dimensional kinetic energy is 0.5. The model uses a time-step of 0.001 seconds, and the results shown here use a snapshot of the velocity fields at 10 seconds, after turbulence has developed but before it has fully decayed. The vorticity calculated from these velocity fields is shown in Figure 1a. The model's vorticity equation includes a hyper-viscosity to ensure numerical stability.

Figure 1 shows a snapshot of the vorticity and its advection term ($\mathcal{A}_\omega$) from the 2D turbulence simulation. $\mathcal{A}_\omega$ is more intermittent than $\omega$ because the former contains derivatives of the vorticity field. This is a simulation of decaying turbulence, and it does not develop a clear inertial cascade of either enstrophy or kinetic energy. As a result, the simulation presents an opportunity to directly compare the scale-dependence and noise-levels of the different structure functions that could be utilized to diagnose the properties of turbulent 2D flows, without making assumptions about the presence of a specific cascade as typical in analytic comparisons. Structure functions are diagnosed by calculating differences ($\delta$ terms) and their correlations for every pair of grid-points in their closest direction, to account for the domain's periodicity. These quantities are binned based on their separation distance into linearly-spaced $r$-bins, and the values within each bin are averaged to calculate structure functions.

Several relations between different structure functions have been presented here. In homogeneous, incompressible 2D turbulence the following relations hold,

$$\overline{\delta\omega\delta\mathcal{A}_\omega} = -\frac{1}{2}\nabla_r\cdot(\overline{\delta\mathbf{u}\delta\omega\delta\omega}), \tag{20}$$

$$\overline{\delta\mathbf{u}\cdot\delta\left(\mathbf{u}\times\boldsymbol{\omega}\right)} = \overline{\delta\mathbf{u}\cdot\delta\boldsymbol{\mathcal{A}_u}} = -\frac{1}{2}\nabla_r\cdot\left(\overline{\delta\mathbf{u}\left(\delta\mathbf{u}\cdot\delta\mathbf{u}\right)}\right). \tag{21}$$

The structure functions in Eq. 20 are both proportional to the inertial cascade rate in the enstrophy cascade of 2D turbulence. More generally, Eq. 20 applies in any 2D isotropic homogeneous flow. However, with finite data sets the left- and right-hand sides of Eq. 20 may not be exactly equivalent. Figure 2a-b shows these structure

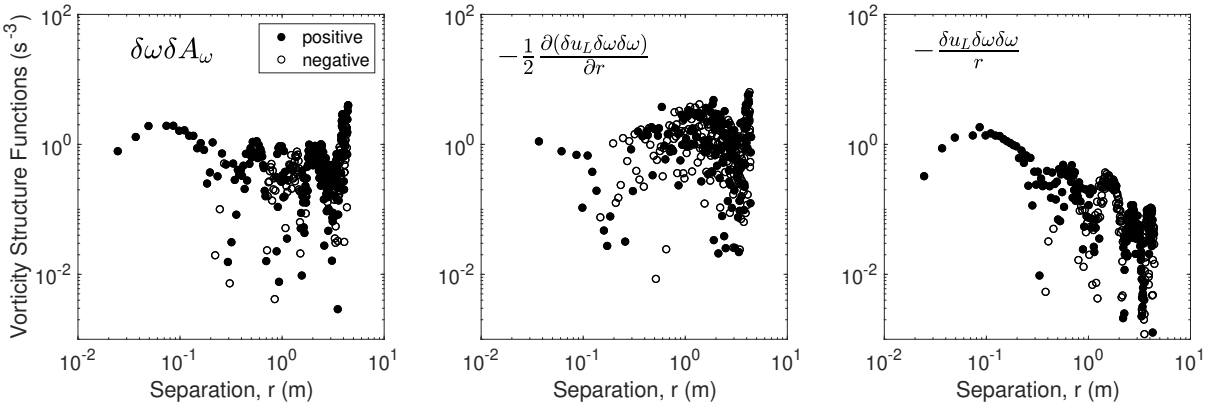


FIG. 2 Vorticity-based structure functions diagnosed from freely-decaying 2D turbulence. Shown are the magnitude of (left) $\overline{\delta\omega\delta\mathcal{A}_\omega}$, (center) $-\frac{1}{2}\nabla_r\cdot(\overline{\delta\mathbf{u}\delta\omega\delta\omega})$, and (right) $-\overline{\delta\mathbf{u}\delta\omega\delta\omega}/r$ as a function of separation distance $r$. Filled symbols denote positive values, while empty symbols denote negative values.

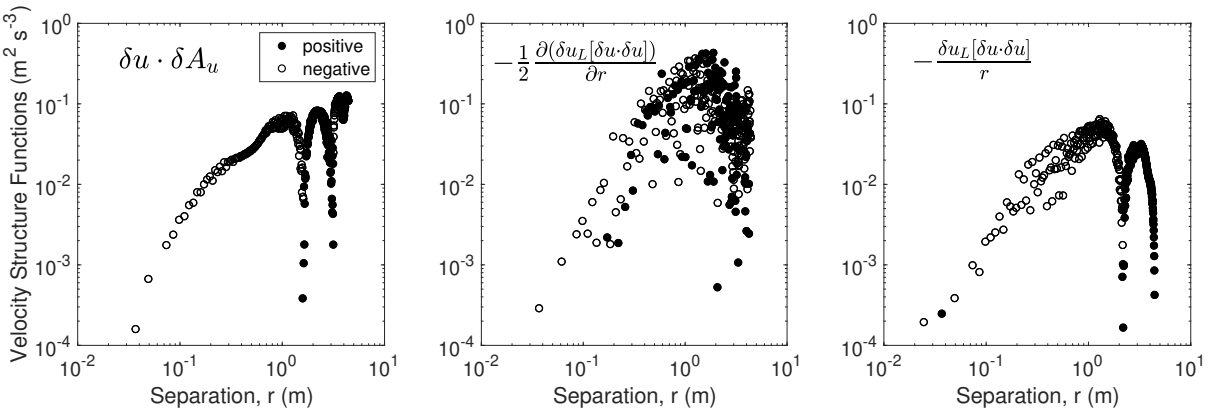


FIG. 3 Velocity-based structure functions diagnosed from freely-decaying 2D turbulence. Shown are the magnitude of (left) $\overline{\delta\mathbf{u}\cdot\delta\boldsymbol{\mathcal{A}}_{\boldsymbol{u}}}$, (center) $-\frac{1}{2}\nabla_r\cdot(\overline{\delta u_L[\delta\mathbf{u}\cdot\delta\mathbf{u}]})$, and (right) $-\overline{\delta u_L[\delta\mathbf{u}\cdot\delta\mathbf{u}]}/r$ as a function of separation distance $r$. Filled symbols denote positive values, while empty symbols denote negative values.

functions, while Figure 3a-b shows the structure functions from Eq. 21. In both cases the magnitude and sign of the new structure functions is similar to the divergence of the third-order structure functions, particularly at small scales. However, the divergence terms are much noisier than the new structure functions, flipping between positive and negative values at intermediate to large scales. This suggests that the new structure functions have different convergence properties relative to the divergence terms, and this could be beneficial for analysis of finite data sets. The derivatives with respect to $r$ were calculated using a centered difference with a 3-bin stencil. Increasing the stencil width did not significantly affect the results.

The analysis of structure function divergences is rare. It is more common to integrate the divergences to find a direct relation to the third-order structure functions. This is possible in turbulence that is also isotropic, where Eqs. 20 and 21 can be integrated over a cylinder of infinitesimal depth and the structure functions are a function of $r$ only. For example, Eq. 21 becomes, after using Gauss' divergence theorem and simplifying,

$$\int_0^r r'\overline{\delta\mathbf{u}\cdot\delta\boldsymbol{\mathcal{A}}_{\boldsymbol{u}}}dr' = -\frac{r}{2}\overline{\delta u_L[\delta\mathbf{u}\cdot\delta\mathbf{u}]}. \tag{22}$$

This demonstrates that the relation between structure functions is governed by the $r$-dependence of $\overline{\delta\mathbf{u}\cdot\delta\boldsymbol{\mathcal{A}}_{\boldsymbol{u}}}$. Equations 17 and 19 suggest potential $r^2$ and $r^0$ dependence for different inertial cascades. Assuming that $\overline{\delta\mathbf{u}\cdot\delta\boldsymbol{\mathcal{A}}_{\boldsymbol{u}}}$ has an arbitrary power law dependence ($r^n$) over a significant range of scales, it follows that,

$$\overline{\delta\mathbf{u}\cdot\delta\boldsymbol{\mathcal{A}}_{\boldsymbol{u}}} \approx -\frac{n+2}{2r}\overline{\delta u_L[\delta\mathbf{u}\cdot\delta\mathbf{u}]}, \tag{23}$$

and similarly from Eq. 20,

$$\overline{\delta\omega\delta\mathcal{A}_\omega} \approx -\frac{n+2}{2r}\overline{\delta u_L\delta\omega\delta\omega}. \tag{24}$$

Equations 23 and 24 are consistent with the new relationships developed here and existing relations for the enstrophy cascade (Eq. 4 versus Eqs. 13 and 17) and inverse KE cascade (Eq. 19 versus Eq. 28 of Lindborg, 1999[11]).

It is clear that neither of the new structure functions have constant slopes across all scales in this simulation

(Figs. 2a and 3a). However, there are regions, particularly at small scales, where they are approximately constant with respect to $r$. As suggested by Eqs. 23 and 24, in these regions the shape and sign of the third-order structure functions normalized by $r$ (Figs. 2c and 3c) is similar to the new structure functions. This relation breaks down at large-scales, where the new structure functions remain similar in magnitude to the divergence, while the third-order structure functions have lower magnitudes. In addition, the third-order velocity structure function (Fig. 3c) has more bin-to-bin variability than the new structure function. This third-order structure function has previously been used as a tool to quantify 2D and quasi-2D dynamics. This means that the new structure functions, which are smoother across scales than the third-order structure functions, could provide a better tool for quantifying flows from finite data sets.

## V. CONCLUSIONS

Two new structure function laws have been derived for the enstrophy cascade of anisotropic, homogeneous 2D turbulence (Eq. 13 and Eq. 16). One of these laws relates a second-order structure function to the enstrophy cascade rate, and in contrast to existing laws it can be evaluated *without* integration. This means that it does not require a prior quantification of flow anisotropy. The results are not affected by a constant background flow or by solid body rotation of the system. The second-order mixed structure functions used here can be related to third-order structure functions. As a result, relationships follow for more complex 2D turbulent systems where third-order structure function laws already exist, such as those with large-scale drag or forcing at a specific scale. A numerical simulation of 2D turbulent flow showed that the new structure functions have smoother profiles as a function or separation distance $r$, than more commonly used structure functions. This suggests that the new structure functions could provide a useful tool for analyzing finite data sets.

## ACKNOWLEDGMENTS

Funding from ONR N00014-17-1-2963 is gratefully acknowledged.

### Appendix A: Coordinate Transformations

The derivation of the correlation equations and structure function relationships requires a coordinate transformation to relative coordinates, $\mathbf{r}$ and $\mathbf{x}_0$, from the Navier-Stokes equation co-ordinates, $\mathbf{x} = \mathbf{x}_0$ and $\mathbf{x}' = \mathbf{x}_0 + \mathbf{r}$. This transformation can be derived from the total derivative of a function $f = f(\mathbf{x}, \mathbf{x}') = f(\mathbf{x}_0, \mathbf{r})$ (for simplicity we assume differences in an arbitrary direction and drop vector notation);

$$df = \left(\frac{\partial f}{\partial x}\right)_{x'} dx + \left(\frac{\partial f}{\partial x'}\right)_{x} dx' = \left(\frac{\partial f}{\partial x_0}\right)_{r} dx_0 + \left(\frac{\partial f}{\partial r}\right)_{x_0} dr, \tag{A1}$$

where subscripts on brackets denote variables that are held constant and $df$ denotes the total differential of $f$. It then follows that, if $x$ is varied while $x'$ is held constant ($dx' = 0 = dx_0 + dr$ and $dx = dx_0$) then,

$$\left(\frac{\partial f}{\partial x}\right)_{x'} = \left(\frac{\partial f}{\partial x_0}\right)_{r} - \left(\frac{\partial f}{\partial r}\right)_{x_0}. \tag{A2}$$

Similarly, if instead $x'$ is varied while $x$ is held constant ($dx = 0 = dx_0$ and $dx' = dx_0 + dr = dr$) then,

$$\left(\frac{\partial f}{\partial x'}\right)_{x} = \left(\frac{\partial f}{\partial r}\right)_{x_0}. \tag{A3}$$

The above two equations demonstrate the co-ordinate transformation of[15]; $\partial/\partial x \rightarrow \partial/\partial x_0 - \partial/\partial r$ and $\partial/\partial x' \rightarrow \partial/\partial r$. The same method can be applied to demonstrate other transformation choices[18]. For example the transform from $r$ and $x_0$ to $x$ and $x'$ is $\partial/\partial r \rightarrow \partial/\partial x'$ and $\partial/\partial x_0 \rightarrow \partial/\partial x + \partial/\partial x'$. In this transformation, if the flow is homogeneous $\partial\overline{f}/\partial x_0 = 0$ for any averaged variable $\overline{f}$, resulting in the additional relations $\partial\overline{f}/\partial x = -\partial\overline{f}/\partial x'$ and $\partial\overline{f}/\partial r = -\partial\overline{f}/\partial x$. Note that $f$ in this case can be a function of both primed and unprimed variables.

[a] Electronic mail: brodie_pearson@brown.edu

[12] G. Falkovich, K. Gawdzki, and M. Vergassola, "Particles and fields in fluid turbulence," Reviews of modern Physics **73**, 913 (2001).

[22] F. Feraco, R. Marino, A. Pumir, L. Primavera, P. D. Mininni, A. Pouquet, and D. Rosenberg, "Vertical drafts and mixing in stratified turbulence: Sharp transition with froude number," EPL (Europhysics Letters) **123**, 44002 (2018).

[a] Electronic mail: brodie_pearson@brown.edu

[1] A. N. Kolmogorov, "The local structure of turbulence in incompressible viscous fluid for very large reynolds numbers," in *Dokl. Akad. Nauk SSSR*, Vol. 30 (1941) pp. 299–303.

[2] U. Frisch, *Turbulence* (Cambridge Univ. Press, 1995).

[3] J. J. Podesta, "Laws for third-order moments in homogeneous anisotropic incompressible magnetohydrodynamic turbulence," Journal of Fluid Mechanics **609** (2008), 10.1017/S0022112008002280.

[4] S. Galtier, "Exact vectorial law for axisymmetric magnetohydrodynamics turbulence," The Astrophysical Journal **704**, 1371 (2009).

[5] S. Galtier, "Exact vectorial law for homogeneous rotating turbulence," Phys. Rev. E **80**, 046301 (2009).

[6] P. Augier, S. Galtier, and P. Billant, "Kolmogorov laws for stratified turbulence," Journal of Fluid Mechanics **709**, 659–670 (2012).

[7] S. Galtier, "Third-order elsässer moments in axisymmetric mhd turbulence," C. R. Phys. **12**, 151–159 (2011).

[8] S. Banerjeeand S. Galtier, "An alternative formulation for exact scaling relations in hydrodynamic and magnetohydrodynamic turbulence," J. Phys. A-Math. Theor. **50**, 015501 (2016).

[9] J. Podesta, M. Forman, C. Smith, D. Elton, Y. Malécot, and Y. Gagne, "Accurate estimation of third-order moments from turbulence measurements," Nonlinear Processes in Geophysics **16**, 99 (2009).

[10]J. Duchonand R. Robert, "Inertial energy dissipation for weak solutions of incompressible Euler and Navier-Stokes equations," Nonlinearity **13**, 249–255 (2000).

[11]E. Lindborg, "Can the atmospheric kinetic energy spectrum be explained by two-dimensional turbulence?" J. Fluid Mech. **388**, 259–288 (1999).

[12]G. Falkovich, K. Gawdzki, and M. Vergassola, "Particles and fields in fluid turbulence," Reviews of modern Physics **73**, 913 (2001).

[13]E. Lindborg, "A note on Kolmogorov's third-order structure-function law, the local isotropy hypothesis and the pressure–velocity correlation," Journal of Fluid Mechanics **326**, 343 (1996).

[14]J. Y. N. Choand E. Lindborg, "Horizontal velocity structure functions in the upper troposphere and lower stratosphere: 1. Observations," Journal of Geophysical Research: Atmospheres **106**, 10223–10232 (2001).

[15]E. Lindborgand J. Y. N. Cho, "Horizontal velocity structure functions in the upper troposphere and lower stratosphere: 2. Theoretical considerations," Journal of Geophysical Research: Atmospheres **106**, 10233–10241 (2001).

[16]E. Deusebio, P. Augier, and E. Lindborg, "Third-order structure functions in rotating and stratified turbulence: a comparison between numerical, analytical and observational results," Journal of Fluid Mechanics **755**, 294–313 (2014).

[17]P. B. Rhines, "Waves and turbulence on a beta-plane," J. Fluid Mech. **69**, 417–443 (1975).

[18]E. Lindborg, "A Helmholtz decomposition of structure functions and spectra calculated from aircraft data," Journal of Fluid Mechanics **762** (2015), 10.1017/jfm.2014.685.

[19]R. T. Cerbusand P. Chakraborty, "The third-order structure function in two dimensions: The Rashomon effect," Physics of Fluids **29**, 111110 (2017).

[20]A. F. Thompsonand W. R. Young, "Scaling baroclinic eddy fluxes: Vortices and energy balance," J. Phys. Oceanogr. **36**, 720–738 (2006).

[21]J.-H. Xieand O. Bühler, "Exact third-order structure functions for two-dimensional turbulence," J. Fluid Mech. **851**, 672–686 (2018).

[22]F. Feraco, R. Marino, A. Pumir, L. Primavera, P. D. Mininni, A. Pouquet, and D. Rosenberg, "Vertical drafts and mixing in stratified turbulence: Sharp transition with froude number," EPL (Europhysics Letters) **123**, 44002 (2018).

[23]D. Balwada, J. H. LaCasce, and K. G. Speer, "Scale-dependent distribution of kinetic energy from surface drifters in the gulf of mexico," Geophys. Res. Lett. **43** (2016).

[24]A. C. Poje, T. M. Özgökmen, D. J. Bogucki, and A. Kirwan, "Evidence of a forward energy cascade and Kolmogorov self-similarity in submesoscale ocean surface drifter observations," Phys. Fluids **29**, 020701 (2017).

[25]J. LaCasce, "Statistics from Lagrangian observations," Progress in Oceanography **77**, 1–29 (2008).

[26]H. Chang, H. S. Huntley, A. D. Kirwan Jr., D. F. Carlson, J. A. Mensa, S. Mehta, G. Novelli, T. M. Özgökmen, B. Fox-Kemper, B. C. Pearson, J. L. Pearson, R. R. Harcourt, and A. C. Poje, "Small-scale dispersion in the presence of Langmuir turbulence," J. Phys. Oceanogr. (2019).

[27]J. Pearson, B. Fox-Kemper, R. Barkan, J. Choi, A. Bracco, and J. C. McWilliams, "Impacts of convergence on structure functions from surface drifters in the Gulf of Mexico," J. Phys. Oceanogr. **49**, 675–690 (2019).

[28]J. C. Ohlman, M. J. Molemaker, B. Baschek, B. Holt, G. Marmorino,and G. Smith, "Drifter observations of submesoscale flow kinematics in the coastal ocean," Geophys. Res. Lett. **44**, 330–337 (2017).

[29]J. Pearson, B. Fox-Kemper, B. Pearson, H. Chang, B. K. Haus, J. Horstmann, H. S. Huntley, A. D. Kirwan, B. Lund,and A. Poje, "Biases in structure functions from observations of submesoscale flows," Under Review.

[30]H. Khatri, J. Sukhatme, A. Kumar,and M. K. Verma, "Surface ocean enstrophy, kinetic energy fluxes, and spectra from satellite altimetry," J. Geophys. Res. **123**, 3875–3892 (2018).

[31]E. D. Zaronand C. B. Rocha, "Internal Gravity Waves and Meso/Submesoscale Currents in the Ocean: Anticipating High-Resolution Observations from the SWOT Swath Altimeter Mission," B. Am. Meteorol. Soc. **99**, ES155–ES157 (2018).

[32]B. C. Pearson, B. Fox-Kemper, S. Bachman, and F. Bryan, "Evaluation of scale-aware subgrid mesoscale eddy models in a global eddy-rich model," Ocean Model. (2017).

[33]B. C. Pearsonand B. Fox-Kemper, "Log-normal turbulence dissipation in global ocean models," Phys. Rev. Lett. **120**, 094501 (2018).

[34]R. Abernathey, C. B. Rocha, F. J. Poulin, M. Jansen, and J. Penn, "pyqg: v0.2.0 (Version v0.2.0). Zenodo. http://doi.org/10.5281/zenodo.50569,".

[35]J. C. McWilliams, "The emergence of isolated coherent vortices in turbulent flow," J. Fluid Mech. **146**, 21–43 (1984).